2011 50th IEEE Conference on Decision and Control and
European Control Conference (CDC-ECC)
Orlando, FL, USA, December 12-15, 2011

Direct Continuous Time System Identification of MISO Transfer Function Models applied to Type 1 Diabetes

Harald Kirchsteiger, Stephan Pölzer, Rolf Johansson, Eric Renard, Luigi del Re

Abstract— **This paper shows an application of continuous time system identification methods to Type 1 diabetes. First, a general MISO transfer function structure with individual nominator and denominator polynomials for each input is assumed and a parameter estimation procedure via an iterative prediction error method presented. Then, the proposed identification method is evaluated on a simple simulation example and finally applied on real-life data from Type 1 diabetes patients with the purpose of modeling blood glucose dynamics. To this aim, the method was extended to consider the time-varying nature of the system.**

I. INTRODUCTION

There are several advantages of continuous time (CT) system identification compared to discrete time (DT) system identification, e.g., data do not need to be sampled equidistantly [1] and the parameters of the estimated models can be interpreted according to their physical meaning, giving insight into the process under consideration [2]. When a physically motivated CT model structure is transformed into DT, the DT parameters are functions of the CT parameters and the sample time, and in general there is no unique re-transformation.

One may distinguish between direct and indirect CT identification methods, where in the latter case DT models are estimated using standard techniques [3] [4] and transformed afterwards into CT, rising problems like the correct transformation of system zeros as mentioned in [5]. An overview of existing algorithms and their comparison was given in [6] focusing on transfer function system representations. The CT state space identification approach was considered in [7]. More recent developments are instrumental variables (IV) techniques to identify MISO transfer functions with individual denominator polynomials [8] and errors in variables methods [9].

This paper presents a way of identifying MISO transfer function models in Section 2. We assume an output error structure although we do not take directly into account the effect of noise as treated e.g. in [5]. The method is validated in a simulation example in Section 3 and thereafter applied to a real-world problem, the identification of blood glucose (BG) traces of Type 1 diabetes patients in Section 4.

H. Kirchsteiger, S. Pölzer and L. del Re are with the Institute for Design and Control of Mechatronical Systems, Johannes Kepler University Linz, 4040 Linz, Austria {harald.kirchsteiger, stephan.poelzer, luigi.delre}@jku.at, http://desreg.jku.at

R. Johansson is with the Department of Automatic Control, Lunds Universitet, Lund, Sweden. rolf.johansson@control.lth.se

E. Renard is with the Endocrinology Department, University Hospital & University of Montpellier 1, Montpellier, France. e-renard@chu-montpellier.fr

There has been a strong effort in modeling blood glucose dynamics from Type 1 diabetes patients in the last centuries, mainly driven by the quest for the artificial pancreas [10]. This system should automatically deliver the correct dosage of insulin (control variable) into the subcutaneous tissue in order to reach a target of the BG concentration (controlled output). Advanced control strategies such as model predictive control, which was intensively analyzed in this context [11] [12] require accurate simulation models or at least prediction models with horizons in the magnitude of the dominant system dynamics which is several hours. The modeling effort was devoted to both physiology based modeling [13] and pure data based modeling [14] [15].

The complexity of the human body, non-repeatable measurement conditions and the very limited availability of long term, high quality measurement data of single patients are—among other reasons [10]—the major difficulties and reasons why until now, no simulation models tuned to single patients are validated with reasonable accuracy. See e.g., [16] for an overview of diabetes signals, modeling and control.

One major premise in successfully applying system identification techniques is the persistent excitation (PE) property of the input signals. Here, the two most important inputs—food intake and insulin injection—usually appear at almost the same time and can be considered as single impulses in time, which means they are not PE of any order. This might be a reason—at least it is the experience of the authors—why many data based modeling approaches result in accurate short term predictions but fail to give reasonable long term predictions. Analyzing those models it can be frequently seen that impulse responses from a carbohydrate or insulin input to an blood glucose output are not compatible with physiology and clinical practice—either in the magnitude or the time scale—or the inputs even do not have any effect on the output. In those cases the high predictive performance is achieved solely through an auto-regressive part in the model.

Here, we chose the CT system identification approach because of two reasons: it is guaranteed that the impulse inputs have an effect on the output and due to the assumed model structure, the estimated parameters can be directly linked to physiological parameters which are of high significance in BG control design, the insulin sensitivity and the carbohydrate sensitivity.

II. MISO SYSTEM IDENTIFICATION ALGORITHM

Consider the description of a system (1) with n_u inputs, $u^{(1)}(t), \ldots, u^{(n_u)}(t),\ t \in \mathbb{R}$ and the polynomials defined according to (2) where n_{ai} and n_{bi} is the maximum order

978-1-61284-799-3/11/$26.00 ©2011 IEEE

of the $A^{(i)}(p)$– and $B^{(i)}(p)$ polynomial, respectively.

$$\hat{y}(t) = \frac{B^{(1)}(p)}{A^{(1)}(p)}u^{(1)}(t) + \cdots + \frac{B^{(n_u)}(p)}{A^{(n_u)}(p)}u^{(n_u)}(t) \quad (1)$$

$$A^{(i)}(p) = 1 + a_1^{(i)}p + \cdots + a_{n_{ai}}^{(i)}p^{n_{ai}} \quad (2a)$$

$$B^{(i)}(p) = b_0^{(i)} + b_1^{(i)}p + \cdots + b_{n_{bi}}^{(i)}p^{n_{bi}}, \quad i = 1 \dots n_u \quad (2b)$$

Here, we make use of the differential operator p, defined by $px(t) = dx(t)/dt$.

Note that beside the nominator also the denominator polynomials are allowed to be individual for each input and the maximum order of the polynomials, n_a and n_b can also be different for each input, hence we introduce the notation n_{ai} and n_{bi}. The problem considered is to find a parameter vector (3) that minimizes the criterion (4), where ϵ is the difference between measurements and the output of the proposed model structure, evaluated at the (discrete) time instances $k \in \mathbb{Z}$ where measurements are available with N being the total number of measurements.

$$\theta = \begin{bmatrix} {\theta^{(1)}}^T & \dots & {\theta^{(n_u)}}^T \end{bmatrix}^T \quad (3a)$$

$$\theta^{(i)} = \begin{bmatrix} a_1^{(i)} \cdots a_{n_{ai}}^{(i)} \; b_0^{(i)} \cdots b_{n_{bi}}^{(i)} \end{bmatrix}^T, \quad i = 1 \dots n_u \quad (3b)$$

$$J = \sum_{k=1}^{N} \epsilon^2(k, \theta) \quad (4)$$

Assuming an output error structure (5), where $y(t)$ denotes the measured process output, we can write the equation error as (6).

$$y(t) = \hat{y}(t) + \epsilon(t) \quad (5)$$

$$\begin{aligned} A^{(1)}(p) \cdots A^{(n_u)}(p)\epsilon(t,\theta) = {} & A^{(1)}(p) \cdots A^{(n_u)}(p)y(t) \\ & - A^{(2)}(p) \cdots A^{(n_u)}(p)B^{(1)}(p)u^{(1)}(t) - \cdots \\ & - A^{(1)}(p) \cdots A^{(n_u-1)}(p)B^{(n_u)}(p)u^{(n_u)}(t) \end{aligned} \quad (6)$$

A standard method to minimize criterion (4) is the Gauss Newton Algorithm [3], (7) where j indicates the iteration step and the step length α_j may change in every iteration.

$$\begin{aligned} \hat{\theta}^{(j+1)} = {} & \hat{\theta}^{(j)} + \alpha_j \left(\sum_{k=1}^{N} \psi(k, \hat{\theta}^{(j)}) \psi^T(k, \hat{\theta}^{(j)}) \right)^{-1} \\ & \sum_{k=1}^{N} \psi(k, \hat{\theta}^{(j)}) \epsilon(k, \hat{\theta}^{(j)}) \end{aligned} \quad (7)$$

The method makes use of a gradient ψ which can be calculated straightforward under the model assumption (1) via (8).

$$\psi(k, \hat{\theta}) = -\left(\frac{\partial \epsilon(t,\theta)}{\partial \theta} \right)^T \Big|_{t=k, \theta=\hat{\theta}} \quad (8)$$

Taking the partial derivatives of (6) with respect to all model parameters allows us to find the components of the gradient (8) which are described in a condensed way in (9) for $h = 0 \dots n_{bi}$ and (10) for $h = 1 \dots n_{ai}$. Both equations are valid for all inputs, $i = 1 \dots n_u$.

$$\frac{\partial \epsilon(t,\theta)}{\partial b_h^{(i)}} = -\frac{1}{A^{(i)}(p)} \frac{\partial B^{(i)}(p)}{\partial b_h^{(i)}} u^{(i)}(t) \quad (9)$$

$$\frac{\partial \epsilon(t,\theta)}{\partial a_h^{(i)}} = y^{F,i}(t,\theta) - \epsilon^{F,i}(t,\theta) - \sum_{l=1}^{n_u, l \neq i} u^{(l)F}(t) \quad (10)$$

Computing the gradients with respect to the model parameters $a_h^{(i)}$ involves the filter operations (11).

$$y^{F,i}(t,\theta) = \frac{1}{A^{(i)}(p)} \frac{\partial A^{(i)}(p)}{\partial a_h^{(i)}} y(t) \quad (11a)$$

$$\epsilon^{F}(t,\theta) = \frac{1}{A^{(i)}(p)} \frac{\partial A^{(i)}(p)}{\partial a_h^{(i)}} \epsilon(t,\theta) \quad (11b)$$

$$u^{(l)F}(t,\theta) = \frac{1}{A^{(l)}(p)A^{(i)}(p)} \frac{\partial A^{(i)}(p)}{\partial a_h^{(i)}} B^{(l)}(p)u^{(l)}(t) \quad (11c)$$

To robustify the iterative search algorithm (7), a regularization factor $\lambda \in \mathbb{R}^+$ multiplied by an identity matrix I of proper dimension is added (12).

$$\begin{aligned} \hat{\theta}^{(j+1)} = {} & \hat{\theta}^{(j)} + \alpha_j \left(\sum_{k=1}^{N} \psi(k, \hat{\theta}^{(j)}) \psi^T(k, \hat{\theta}^{(j)}) + \lambda I \right)^{-1} \\ & \sum_{k=1}^{N} \psi(k, \hat{\theta}^{(j)}) \epsilon(k, \hat{\theta}^{(j)}) \end{aligned} \quad (12)$$

III. SIMULATION EXAMPLE

The algorithm outlined in the previous section is now applied to a process defined by (13).

$$y(t) = \frac{K_1}{(1+T_1p)^2p}u^{(1)}(t) + \frac{K_2}{(1+T_2p)^2p}u^{(2)}(t) + e(t) \quad (13)$$

The process parameters $\theta = (K_1,\ K_2,\ T_1,\ T_2)^T$ along with the estimates for different noise levels are summarized in Table I. The table shows the estimated parameter values and standard deviations after 50 iterations of the Gauss Newton algorithm for different noise covariances η and the corresponding signal to noise ratio (SNR). For this comparison, two rectangular signals of 150s length, sampled at 5 Hz with $u^{(1)}$ having an amplitude of 0.5 and period 30s and $u^{(2)}$ having an amplitude of 1 and period 20s were used as inputs and $e(t) \sim N(0, \eta^2)$. As initial parameter estimate, we chose $\hat{\theta}^{(0)} = (0.1,\ -0.1,\ 0.1,\ 0.1)^T$, the regularization parameter λ was 0.2 and mean values of 20 Monte Carlo simulations with individual noise realizations are presented. The chosen value for λ decreased the dependency of the results on the initial parameter values and still maintained almost the same performance as if no regularization would be used. A graphical representation is given in Fig.1. The results give evidence that the method can give accurate parameter estimates under the reported conditions.

One might notice that (13) does not exactly lie within the structure defined in (1), as we assumed monic denominator polynomials. To represent an integral behavior, the term 1

TABLE I

SIMULATION EXAMPLE RESULTS

Parameter	True Value	$\eta = 0.1$ SNR= 72.9dB	$\eta = 0.5$ SNR= 43.9dB	$\eta = 1.0$ SNR= 32.9dB
K_1	1	1.0002 (±0.0022)	1.0050 (±0.0104)	1.0016 (±0.0270)
K_2	-2	-2.0001 (±0.0017)	-2.0036 (±0.0086)	-1.9987 (±0.0220)
T_1	2	1.9999 (±0.0036)	2.0165 (±0.0282)	2.0227 (±0.0837)
T_2	4	3.9999 (±0.0042)	4.0053 (±0.0207)	4.0040 (±0.0436)

in (2a) has to be replaced by an additional parameter $a_0^{(i)}$ which makes the transfer function non-univoke, or directly set $a_0^{(i)}$ to zero, what we did here. In this case, the gradients involved in the computation of (12) are given in (14). The reason for choosing this specific transfer function for our simulation example is explained in the following section.

$$\frac{\partial \epsilon(t,\theta)}{\partial K_1} = -\frac{1}{(1+T_1 p)^2 p} u^{(1)}(t) \quad (14a)$$

$$\frac{\partial \epsilon(t,\theta)}{\partial K_2} = -\frac{1}{(1+T_2 p)^2 p} u^{(2)}(t) \quad (14b)$$

$$\frac{\partial \epsilon(t,\theta)}{\partial T_1} = -\frac{2K_2}{(1+T_1 p)(1+T_2 p)^2} u^{(2)}(t) + \frac{2p}{(1+T_1 p)} \left(y(t) - \epsilon(t,\theta)\right) \quad (14c)$$

$$\frac{\partial \epsilon(t,\theta)}{\partial T_2} = -\frac{2K_1}{(1+T_1 p)^2 (1+T_2 p)} u^{(1)}(t) + \frac{2p}{(1+T_2 p)} \left(y(t) - \epsilon(t,\theta)\right) \quad (14d)$$

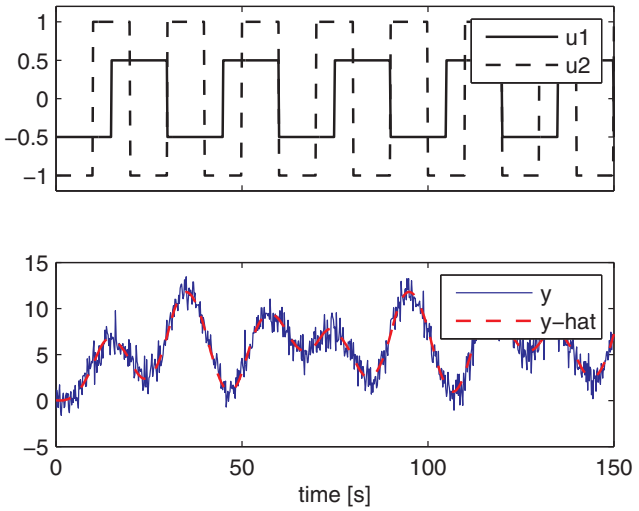

Fig. 1. Simulation example: inputs (upper panel) and simulated model output vs. noisy ($\eta = 1$) measurements (bottom panel)

IV. APPLICATION: MODELING TYPE 1 DIABETES

In [17] it was shown that a reduced order linear transfer function of the form (13) with the inputs $u^{(1)}(t)$ representing the carbohydrate amount ingestion and $u^{(2)}(t)$ the fast acting insulin quantity injected in the subcutaneous tissue is well suited to capture the main blood glucose dynamics after breakfast. Furthermore the parameter K_1 is directly linked to the carbohydrate sensitivity—the BG change after a 1g carbohydrate meal—and K_2 to the insulin sensitivity—the BG change after injection of 1 insulin unit—two parameters that are of uttermost importance for calculating the correct insulin advice for diabetes therapy.

Here, we use data collected from 15 Type 1 diabetes patients over a period of three days each recorded at the endocrinology department of the university hospital in Montpellier, France. Details on the clinical protocol, subjects included, datasets and measurement devices can be found in [17]. As model inputs, we used directly the information coming from the patient, the amount of carbohydrates of the meals and the quantity of insulin injected. Both inputs are zero most of the time and appear as single impulses typically 3-6 times per day. We do not use any filter for those impulse inputs when applying the identification algorithm. As output for the model identification, we use the BG measurements performed at times $t_m = \{0, 10, 20, 30, 45, 60, 90, 120\}$ after a meal using a Hemocue®glucometer.

A. Modeling individual responses

Straightforward application of the algorithm described in the previous section to single meal responses gives results as presented in Fig. 2. for one individual. The signals referred to as measurements are the spline-interpolated discrete BG measurements in whole blood at non-uniform sample intervals. Responses are due to ingestion of a 45g carbohydrate breakfast (mixed meal) and insulin injection based on patients own decision. The high intra-patient variability is evident in the estimated parameter values for the 3 breakfasts on 3 different days (15).

$$\theta_{d1} = \begin{bmatrix} 5.47 \\ -69.29 \\ 20.79 \\ 62.86 \end{bmatrix} \quad \theta_{d2} = \begin{bmatrix} 4.38 \\ -48.35 \\ 18.27 \\ 70.42 \end{bmatrix} \quad \theta_{d3} = \begin{bmatrix} 5.65 \\ -76.44 \\ 20.59 \\ 56.28 \end{bmatrix} \quad (15)$$

B. Modeling collective responses

Focusing on breakfasts, the parameter vectors should be at least similar up to the extent of the day to day variability, as patients received identical meals for the 3 days. To tighten the parameter estimates, several responses of one patient are considered at the same time with additional constraints on the parameter estimates. Instead of criterion (4) we now make use of (16) in the case of an estimation for 2 days. The parameters θ_{d1} are those estimated for the first day and θ_{d2} those for the second day. The cost function (16) can be easily extended to more days. The additional penalty on the parameter differences with a weight as defined in (17) is used to reduce the distance between the parameter vectors for the different days. Note that we still assume different parameter vectors for different experiments which makes the method different than a multi-experiment identification.

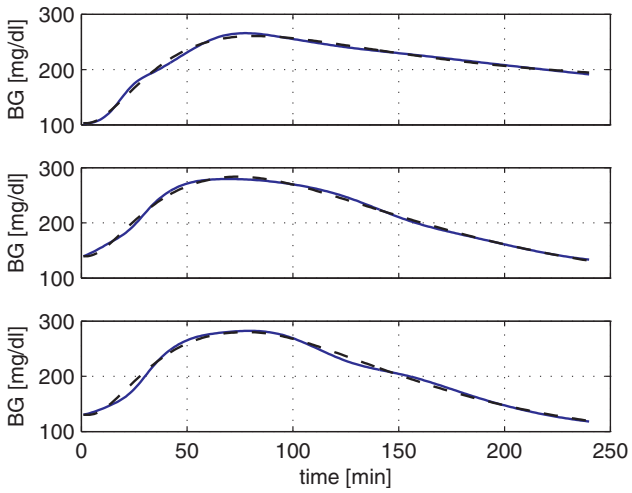

Fig. 2. Simulated model outputs (black dashed) compared with BG measurements (blue solid) for 3 breakfasts of one individual (P0103)

By increasing a specific entry in (17) we can enforce the parameter related to it to be more close for all experiments than the other parameters.

$$\begin{aligned} J &= \sum_{k=1}^{N} \epsilon_{d1}^2(k,\theta_{d1}) + \sum_{k=1}^{N} \epsilon_{d2}^2(k,\theta_{d2}) \\ &\quad + 2p^T(\theta_{d1}-\theta_{d2})^2 \qquad (16) \\ p &= \begin{bmatrix} p_{K1} & p_{K2} & p_{T1} & p_{T2} \end{bmatrix}^T \qquad (17) \end{aligned}$$

A multi-experiment optimization like this—one experiment is equivalent to one meal—is easily incorporated in the framework of the algorithm in Section II as it results in a decoupled optimization problem with the only interconnection being the additional penalty on the distance of the parameter estimates. Specifically, gradients are calculated similarly to (14) for both experiments with the difference that now one constant—in the sense of time-invariant—term according to the parameter penalty has to be added per component. This term is given in (18) and the gradient is (19).

$$\psi_p(\theta_{d1},\theta_{d2}) = 4 \begin{bmatrix} p_{K1}\left(K_1^{d1}-K_1^{d2}\right) \\ p_{K2}\left(K_2^{d1}-K_2^{d2}\right) \\ p_{T1}\left(T_1^{d1}-T_1^{d2}\right) \\ p_{T2}\left(T_2^{d1}-T_2^{d2}\right) \end{bmatrix} \qquad (18)$$

$$\psi(k,\theta_{d1},\theta_{d2}) = \begin{bmatrix} \frac{\partial \epsilon_{d1}(k,\theta_{d1})}{\partial \theta_{d1}} + \psi_p(\theta_{d1},\theta_{d2}) \\ \frac{\partial \epsilon_{d2}(k,\theta_{d2})}{\partial \theta_{d2}} - \psi_p(\theta_{d1},\theta_{d2}) \end{bmatrix} \qquad (19)$$

In the following, we will denote with ψ_1 the first element and with ψ_2 the second element of (19). Substituting (19) into (12) and extension to the 2 experiment case leads to (20) where the Hessian Matrix H is defined according to (21) and f as in (22).

$$\begin{bmatrix} \hat{\theta}_{d1}^{(j+1)} \\ \hat{\theta}_{d2}^{(j+1)} \end{bmatrix} = \begin{bmatrix} \hat{\theta}_{d1}^{(j)} \\ \hat{\theta}_{d2}^{(j)} \end{bmatrix} + \alpha_j \left(H+\lambda I\right)^{-1} + f \qquad (20)$$

TABLE II

INDIVIDUAL VS COLLECTIVE MODEL PARAMETERS

Individual Modeling					
	Day1	Day2	Day3	mean	STD
K_1	3.26	16.55	9.79	9.87	6.64
K_2	-254.42	-187.54	-78.89	-173.62	88.59
T_1	22.77	26.20	22.00	23.65	2.24
T_2	425.70	30.43	31.99	162.71	227.76
Collective Modeling					
	Day1	Day2	Day3	mean	STD
K_1	7.66	6.36	8.71	7.58	1.18
K_2	-67.80	-68.81	-69.96	-68.86	1.08
T_1	34.18	21.58	20.99	25.58	7.45
T_2	49.11	34.35	33.47	38.98	8.78

$$H = \begin{bmatrix} H_{11} & 0 \\ 0 & H_{22} \end{bmatrix} = \begin{bmatrix} \sum_{k=1}^{N} \psi_1 \psi_1^T & 0 \\ 0 & \sum_{k=1}^{N} \psi_2 \psi_2^T \end{bmatrix} \qquad (21)$$

$$f = \begin{bmatrix} \sum_{k=1}^{N} \psi_1 \epsilon_{d1}(k,\theta_{d1}) \\ \sum_{k=1}^{N} \psi_2 \epsilon_{d2}(k,\theta_{d2}) \end{bmatrix} \qquad (22)$$

As per experiment essentially 4 more gradients have to be calculated and one symmetric matrix of dimension 4 inverted, these multiple experiment extensions do not significantly increase the computational cost. Note that the Hessian can be inverted efficiently due to the block-diagonal structure (23).

$$\left(H+\lambda I\right)^{-1} = \begin{bmatrix} \left(H_{11}+\lambda I\right)^{-1} & 0 \\ 0 & \left(H_{22}+\lambda I\right)^{-1} \end{bmatrix} \qquad (23)$$

C. Simulation results on real life data

In general, the methodology of modeling collective responses will give worse results in terms of fitting individual traces than modeling individual responses as performance is traded against a compact parameter set. This is however not always the case, as can be seen in Fig. 3., where the individual model of day 2 (middle panel) optimized according to the prediction error does not capture the peak BG response. In contrast, the collective model captures the peak accurately. In the first two breakfasts (upper and middle panel), the BG concentration first decreases slightly before it starts the increase caused by the meal at $t = 7$ on the first day and $t = 2$ on the second day. This behavior, which can be observed in several of the responses in our database gives evidence that in a future work, the model structure might be extended with a time delay.

Parameter values for both cases are given in Table II for all 3 breakfasts for patient P0111. The simulation results were obtained using a regularization parameter $\lambda = 1$, step size $\alpha_j = 0.075$ and parameter penalty $p = (2,\ 2,\ 0.5,\ 0.5)^T$.

One remaining question is how to make use of the parameter sets for a single patient when the model shall be used for predicting the BG excursions after a meal intake. In this

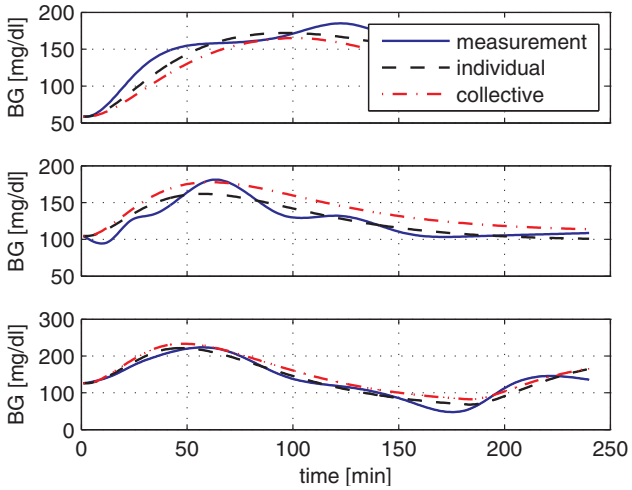

Fig. 3. Simulated model outputs for individual modeling (black dashed) compared with measurements (blue solid) and collective modeling (red dash-dot) for 3 breakfasts of one patient (P0111)

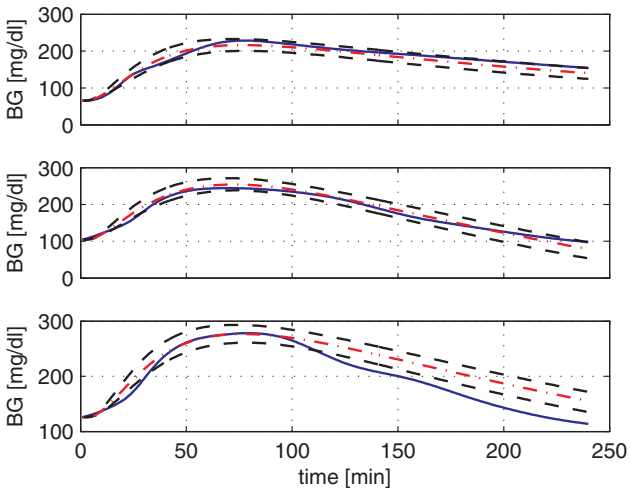

Fig. 4. Simulated "worst case" model outputs (black dashed) compared with measurements (blue solid) and collective modeling (red dash-dot) for 3 breakfasts of one patient (P0107)

case we assume the parameters for a single experiment be unknown. The estimated parameter intervals (24) calculated over several days can be used to compute upper and lower boundaries i.e., worst case scenarios according to (26) and (27). Here, $\underline{\theta} = (\underline{K}_1, \underline{K}_2, \underline{T}_1, \underline{T}_2)$ is the parameter vector constructed of all the individual minimum values of all estimated parameter vectors for dn days, (25); similarly $\overline{\theta}$ consists of all the maximum values.

$$\theta \in \left[\underline{\theta},\ \overline{\theta}\right] \tag{24}$$

$$\underline{\theta} = \begin{bmatrix} \min\{K_1^{d1}, \ldots, K_1^{dn}\} \\ \min\{K_2^{d1}, \ldots, K_2^{dn}\} \\ \min\{T_1^{d1}, \ldots, T_1^{dn}\} \\ \min\{T_2^{d1}, \ldots, T_2^{dn}\} \end{bmatrix} \tag{25}$$

$$\hat{y}_{max}(t) = \frac{\overline{K}_1}{(1+\underline{T}_1 p)^2 p} u^{(1)}(t) + \frac{\underline{K}_2}{(1+\overline{T}_2 p)^2 p} u^{(2)}(t) \tag{26}$$

$$\hat{y}_{min}(t) = \frac{\underline{K}_1}{(1+\overline{T}_1 p)^2 p} u^{(1)}(t) + \frac{\overline{K}_2}{(1+\underline{T}_2 p)^2 p} u^{(2)}(t) \tag{27}$$

An example of such boundaries is given in Fig. 4., again for 3 breakfasts of one patient. Additionally, the response of the model using the collective modeling parameters is given. The bottom panel shows that the measurements do not always lie within the maximum and minimum responses.

V. DISCUSSION

A. Variability

The first property to highlight is the comparatively high variability in the blood glucose responses to meals of similar composition and quantity even in the same patient in consecutive days under hospitalized conditions. Here, we analyzed in total data from 15 patients over a time period of 3 days each, i.e., 3 breakfasts, 3 dinners and 3 lunches for each individual giving in total 135 experiments. Out of this data pool, 20 experiments did not fit into the proposed model class (13) and in 4 experiments data were partially missing. A common problem in clinical data, as some variables like the carbohydrate content of the meal and the insulin quantity administered is written in a log-book and afterwards manually transferred into an electronic format. To account for the intra-day variability we analyzed breakfast lunch and dinner experiments separately. Considering the design of the study, the variability introduced by varying meal components was minimized at breakfast times as the same breakfast was served at all 3 days where as for lunch and dinner meals of comparable size but different nutrients were prescribed.

B. Collective modeling

The remaining 111 experiments gave reasonable results and were considered further in the collective modeling. This approach essentially ties together the parameter estimates of the several days when increasing the tuning parameters in (18) but at the same time decreases the fit of the model output to the data. Simulation results showed that up to some extent, the fit is changing only minimally when imposing the parameter difference penalty with a moderate weight. We justify the approach by considering an application of the model in glucose control, where it is not required neither to achieve accurate setpoint tracking nor to have high dynamic disturbance rejection. This means requirements on the model can be relaxed. The accurate description of the BG peak value and time after a meal when it occurs is already sufficient for patients who deliver insulin via multiple daily injections (typically one injection per mean) to decide on the insulin dose to compensate the meal.

As mentioned before, the regularization parameter λ was constant for all simulations. In a further step, the algorithm might be extended to find an optimal λ for each patient which decreases the performance by a given percentage. Graphically, we are then trying to find a level set of a

given performance in the 4-dimensional parameter space for all experiments. The higher λ, the more likely the various level sets will overlap each other and we can find a unique parameter vector which describes all experiments with the same error. Simulations showed that such a high λ will lead to unacceptable performance and thus smaller values have to be used and the parameter set could be described by the borders of the individual level sets delimited by perpendicular hyperplanes between them.

C. Parameter intervals

Focusing on the breakfast data only, we were able to obtain compact parameter sets for each patient describing the measurements accurately. However, this was not the case for lunch and dinner modeling. In this case the individual parameter vectors for the 3 days typically have a large variability and much of the performance is lost to make them compact. As an example, we present results for the lunch of patient P0109 in Fig. 5. where both the performance of the model to capture the measurements is bad and the difference between minimum and maximum response is big because of a non-compact parameter set. In this particular case, note the BG response on day 3 in the lower panel, which does not increase after the lunch was eaten. Also note that in this case, the patient had a small snack after the lunch at t around 160 min. Consequently, the simulated upper and lower bounds of the BG concentrations change here, whereas the parameter intervals are the same for the whole experiment.

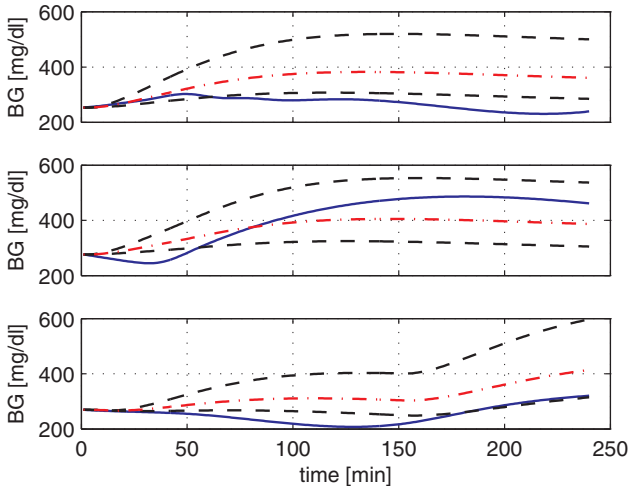

Fig. 5. Simulated "worst case" model outputs (black dashed) compared with measurements (blue solid) and collective modeling (red dash-dot) for 3 lunches of one patient (P0109)

D. Use of the model

Insulin bolus calculators, which are currently clinical standard in intensive insulin therapy calculate insulin needs based on the insulin sensitivity and carbohydrate correction factors. These two factors are directly given by our model assumption. After the model parameters are fixed, a single BG measurement is necessary to determine the offset of the simulated model output. The time of this measurement is the beginning of a meal, where measurements are typically taken. The formulation in terms of parameter intervals might be used in a robust control setup.

VI. ACKNOWLEDGMENTS

The authors gratefully acknowledge the sponsoring of this work by the European Commision through the Information Society Technologies (IST) programme under the Seventh Framework Programme (FP7) n° 216592 in the context of the DIAdvisor project.

REFERENCES

[1] R. Johansson, "Continuous-time model identification and state estimation using non-uniformly sampled data," in *Proc. 19th Int. Symp. Mathematical Theory of Networks and Systems (MTNS2010)*, Budapest, Hungary, 5-9 July 2010, pp. 347–354, invited Paper.

[2] H. Garnier and L. Wang, Eds., *Identification of Continuous Time Models from Sampled Data*. London: Springer, 2008.

[3] T. Söderström and P. Stoica, *System Identification*. Hemel Hempstead, UK: Prentice Hall International, 1989.

[4] R. Johansson, *System Modeling and Identification*. New Jersey: Prentice Hall, 1993.

[5] ——, "Identification of continuous-time models," *IEEE Transactions on Signal Processing*, vol. 42, pp. 887–879, 1994.

[6] H. Garnier, M. Mensler, and A. Richard, "Continuous-time model identification from sampled data: implementation issues and performance evaluation," *International Journal of Control*, vol. 76, pp. 1337–1357, 2003.

[7] R. Johansson, M. Verhaegen, and C. Chou, "Stochastic theory of continuous-time state-space identification," *IEEE Transactions on Signal Processing*, vol. 47, pp. 41–51, 1999.

[8] H. Garnier, M. Gilson, P. Young, and E. Huselstein, "An optimal iv technique for identifying continuous-time transfer function model of multiple input systems," *Control Engineering Practice*, vol. 15, pp. 471–486, 2007.

[9] K. Mahata and H. Garnier, "Identification of continuous-time errors-in-variables models," *Automatica*, vol. 42, pp. 1477–1490, 2006.

[10] R. Harvey, W. Youqing, B. Grosman, M. Percival, W. Bevier, D. Finan, H. Zisser, D. Seborg, L. Jovanovic, I. Doyle, F.J., and E. Dassau, "Quest for the artificial pancreas: Combining technology with treatment," *IEEE Engineering in Medicine and Biology Magazine*, vol. 29, pp. 53–62, 2010.

[11] R. S. Parker, F. J. Doyle III, and N. Peppas, "A model-based algorithm for blood glucose control in type 1 diabetic patients," *IEEE Transactions on Biomedical Engineering*, vol. 46, pp. 148–157, 1999.

[12] L. Magni, D. M. Raimondo, L. Bossi, C. Dalla Man, G. De Nicolao, B. Kovatchev, and C. Cobelli, "Model predictive control of type 1 diabetes: An in silico trial," *Journal of Diabetes Science and Technology*, vol. 1, pp. 804–812, 2007.

[13] C. Dalla Man, R. A. Rizza, and C. Cobelli, "Meal simulation model of the glucose-insulin system," *IEEE Transactions on Biomedical Engineering*, vol. 54, pp. 1740–1749, 2007.

[14] F. Stahl and R. Johansson, "Diabetes mellitus modeling and short-term prediction based on blood glucose measurements," *Mathematical Biosciences*, vol. 217, pp. 101–117, 2009.

[15] G. Castillo Estrada, H. Kirchsteiger, L. Del Re, and E. Renard, "Innovative approach for online prediction of blood glucose profile in type 1 diabetes patients," in *Proc. American Control Conference (ACC), 2010*, Baltimore, Maryland, USA, June 30 - July 2 2010, pp. 2015–2020.

[16] C. Cobelli, C. Dalla Man, G. Sparacino, L. Magni, G. De Nicolao, and B. Kovatchev, "Diabetes: Models, signals and control," *IEEE Reviews in Biomedical Engineering*, vol. 2, pp. 54–96, 2009.

[17] H. Kirchsteiger, G. Castillo Estrada, S. Pölzer, E. Renard, and L. Del Re, "Estimating interval process models for type 1 diabetes for robust control design," in *Proc. 18th IFAC World Congress*, Milano, Italy, August 28 - September 2 2011, pp. 11 761–11 766.